

Automatic Multithreshold Selection

SHYUAN WANG AND ROBERT M. HARALICK

Department of Computer Science and Electrical Engineering, Virginia Polytechnic Institute and State University, Blacksburg, Virginia 24061

Received September 15, 1982; revised October 18, 1982

A recursive technique for multiple threshold selection on digital images is described. Pixels are first classified as edge pixels or nonedge pixels. Edge pixels are then classified, on the basis of their neighborhoods, as being relatively dark or relatively light. A histogram of the graytone intensities is obtained for those pixels which are edge pixels and relatively dark and another histogram is obtained for those pixels which are edge pixels and relatively light. A threshold is selected corresponding to the graytone intensity value corresponding to one of the highest peaks from the two histograms. To get multiple thresholds, the procedure may be recursively applied first using only those pixels whose intensities are smaller than the threshold and then only those pixels whose intensities are larger than the threshold.

1. INTRODUCTION

In image segmentation techniques, nothing is simpler than global thresholding. Two cases are of interest. In case 1, the images simply contain objects and backgrounds; a graytone threshold value is needed to separate them. In case 2, the images contain three or more classes of homogeneous regions; we want to get one "sliced" output image for each of the classes. Case 1 is a special case of case 2. If a graytone image P is defined over a set Z_r of row coordinates, a set Z_c of column coordinates, and a graytone range $[g_1, g_2]$, $P: Z_r \times Z_c \rightarrow [g_1, g_2]$, then the result of case 1 is a two-valued image P_2 , $P_2: Z_r \times Z_c \rightarrow \{0, 1\}$, defined by

$$\begin{aligned} P_2 = 1 &\quad \text{if } P(r, c) > t \\ 0 &\quad \text{if } P(r, c) \leq t, \end{aligned}$$

where t is the graytone threshold and $g_1 < t < g_2$. Similarly, the result of case 2 can be considered as a $(k + 1)$ -valued image P_k , $P_k: Z_r \times Z_c \rightarrow \{0, 1, \dots, k\}$, defined by

$$P_k(r, c) = \begin{cases} k & \text{if } P(r, c) > t(k) \\ k - 1 & \text{if } t(k - 1) < P(r, c) \leq t(k) \\ \vdots & \\ 1 & \text{if } t(2) < P(r, c) \leq t(2) \\ 0 & \text{if } P(r, c) \leq t(1) \end{cases}$$

where $t(i)$, $1 \leq i \leq k$, are thresholds and $g_1 < t(1) < t(2) < \dots < t(k) < g_2$.

A variety of thresholds selection techniques are described in Weszka's [1] survey article. Our method belongs to the class of global threshold selection based on local

properties. There are two ways to use local properties. First, they can be used to modify the graytone histogram. Second, the histogram of local property values can be used directly to compute a global threshold, as suggested by Watanabe et al. [2].

Chow and Kaneko's [3] method is useful when global thresholds are inadequate. In their approach, an image is divided into overlapping windows. Local statistics are measured in each window to determine a threshold. Thresholds for every point in the image are obtained by a linear interpolation procedure. Weszka classifies this method as dynamic threshold selection. The method of this paper could be used to find thresholds within the windows thereby constituting a general segmentation technique.

Two new points of view about using local properties are presented in this paper. First, instead of modifying the graytone histograms, we decompose the histogram of local property values. Second, instead of finding a best binary threshold, we work on the multithreshold selection problem. We believe that more clues are provided in the latter case, leading to a general solution of the threshold selection problem.

In Section 2, Watanabe's experiment is described. In Section 3, we illustrate how to improve Watanabe's result by classifying edge pixels into three categories. In Section 4, a criterion for a good threshold is proposed. In Section 5, an algorithm for multithreshold selection is described. The final two sections are on experimental results and discussion.

2. WATANABE'S METHOD AND SOME VARIATIONS

Watanabe used the gradient approach to determine a global threshold because, at the borders between objects and background, the gradient should be high. If a gradient image is defined as $D: Z_r \times Z_c \rightarrow R^+$ where R^+ is the set of nonnegative real numbers, then the gradient histogram H_1 is defined as $H_1: [g_1, g_2] \rightarrow I^+$, where I^+ is the set of nonnegative integers, and $H_1(g)$ is the sum of the gradient values for all pixels having graytone g , i.e.,

$$H_1(g) = \sum_{(r, c) \in A_1(g)} D(r, c), \quad g \in [g_1, g_2]$$

where $A_1(g) = \{(r, c) | P(r, c) = g \text{ where } P \text{ is the graytone image}\}$.

Watanabe selected graytone t as a threshold where $H_1(t)$ is a peak. In the following, some variations of H_1 are designed to see what effects they might have. The first variation is to use the number of pixels in $A_1(g)$. Thus, histogram $H_2: [g_1, g_2] \rightarrow I^+$ is defined as $H_2(g) = \text{number of pixels in } A_1, g \in [g_1, g_2]$. Another variation [4] is to use the normalized gradient histogram H_3 , $H_3: [g_1, g_2] \rightarrow I^+$, which is defined by $H_3(g) = H_1(g)/H_2(g)$.

In the other variations, we do not use the gradients of all the pixels. A comprehensive comparison of Watanabe's method and four alternatives was reported in [5]. Histograms of pixels having either low or high values were used. Katz [6] suggested producing a histogram of the gray levels of only those pixels that have high edge values. Similarly, we can calculate H_1 , H_2 , H_3 only at locations where "meaningful" edge responses are detected. To do this, we need a binary edge image $E: Z_r \times Z_c \rightarrow \{0, 1\}$, where

$$\begin{aligned} E(r, c) &= 1 && \text{if } (r, c) \text{ is identified as an edge pixel,} \\ &= 0 && \text{otherwise.} \end{aligned}$$

TABLE 2.1
Design of Six Different Histograms

Calculation	Pixel selection	
	All pixels	Edge pixels only
Gradient	H_1	H_4
Number of pixels	H_2	H_5
Normalized gradient	H_3	H_6

Now using the edge image, H_1 , H_2 , H_3 can be modified into H_4 , H_5 , H_6 , where

$$H_4(g) = \sum_{(r, c) \in A_2(g)} D(r, c)$$

$$A_2(g) = \{(r, c) | P(r, c) = g, E(r, c) = 1\},$$

$$H_5(g) = \text{number of pixels in } A_2(g),$$

and

$$H_6(g) = H_4(g)/H_5(g).$$

An experiment using Watanabe's method and variations then has the possibilities shown in Table 2.1. In this experiment, using a Landsat image, we create the image E by Haralick's [7] zero crossing of second directional derivative edge operator which detects good step edges even in noisy pictures. A pixel is identified as an edge pixel if and only if there is some point in the pixel's area having a zero crossing of the second directional derivative taken in the direction of a non-zero gradient at the pixel's center.



FIG. 2.1. Original Landsat image.

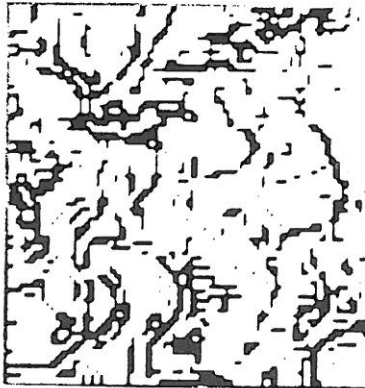


FIG. 2.2. Edge image of Fig. 2.1.

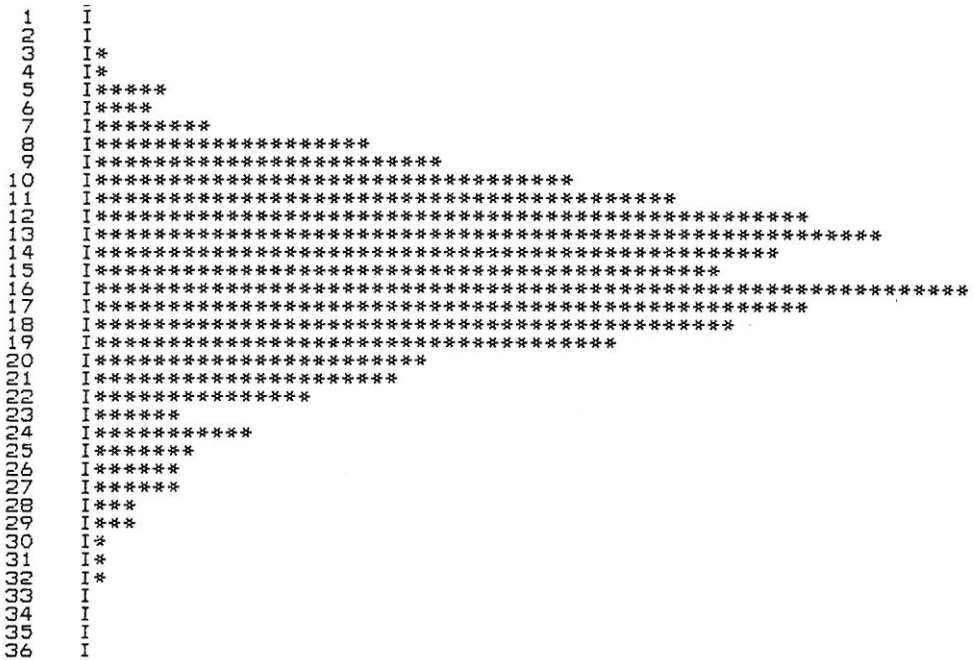
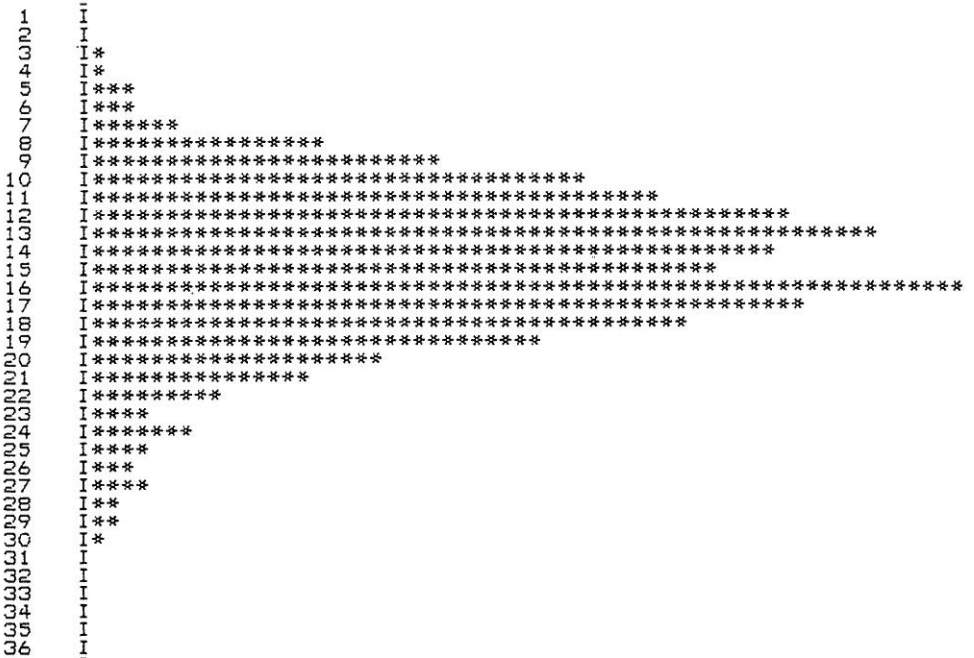
For the Landsat image in Fig. 2.1 and the corresponding binary edge image in Fig. 2.2, the histograms $H_1 \sim H_6$ are shown in Fig. 2.3. From these histograms, it can be concluded that H_1 , H_2 , H_4 , and H_5 are alike, and H_3 , H_6 are not useful. In the following sections, we will concentrate on how to split H_5 to get better results.

3. CLASSIFYING EDGE PIXELS

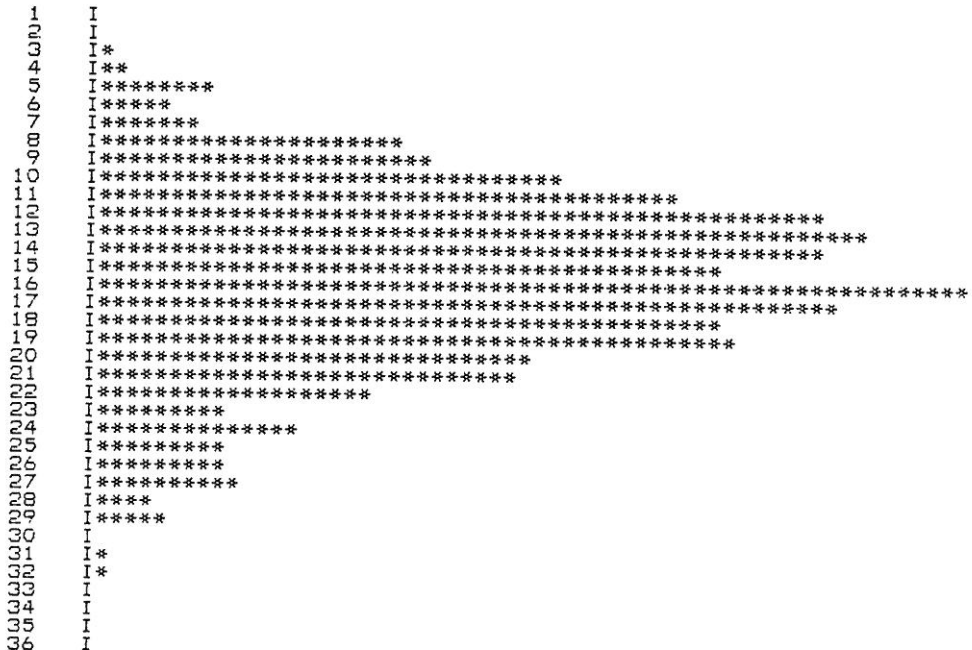
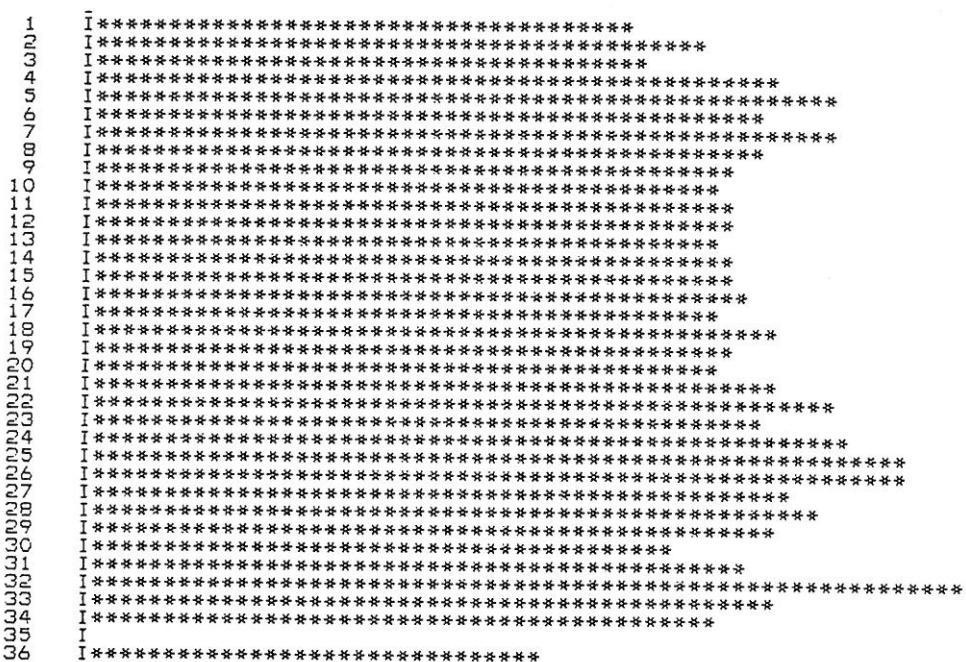
Not all edge pixels in the binary edge image E have the same roles in the relative brightness of the graytone image P . As in Fig. 3.1, edge pixels may be bright (upper plane), dark (lower plane), or gray (slope). Thus, information contained in the above histograms is mixed and ambiguous. One should create another classified edge image $C: Z_r \times Z_c \rightarrow \{0, 1, 2\}$ where

$$\begin{aligned} C(r, c) &= 1 && \text{if edge pixel } (r, c) \text{ is dark compared to} \\ &&& \text{most of its neighbors, or it can be called} \\ &&& \text{a dark edge pixel.} \\ &= 2 && \text{if edge pixel } (r, c) \text{ is bright compared to} \\ &&& \text{most of its neighbors, or it can be called} \\ &&& \text{a bright edge pixel,} \\ &= 0 && \text{otherwise.} \end{aligned}$$

Next, H_5 can be split into H_d and H_b . H_d is the histogram of the dark edge pixels with $H_d(g) = \text{number of elements in } \{(r, c) | P(r, c) = g, C(r, c) = 1\}$. Also H_b is the histogram of numbers of bright edge pixels with $H_b(g) = \text{number of elements in } \{(r, c) | P(r, c) = g, C(r, c) = 2\}$. The histograms for $C(r, c) = 0$ are omitted because they are not interesting. Now, there is a graytone t_1 at which $H_d(t_1)$ is a peak. Also, there is a graytone t_2 at which $H_b(t_2)$ is a peak. It looks as though both t_1 and t_2 could be selected as thresholds, but it should be noted that t_1 and t_2 are totally different ways of getting regions. By thresholding at t_1 , we are supposed to get dark regions, and by thresholding at t_2 , we are supposed to get bright regions. This is the

FIG. 2.3a. Histogram H_1 .FIG. 2.3b. Histogram H_2 .



FIG. 2.3e. Histogram H_5 .FIG. 2.3f. Histogram H_6 .

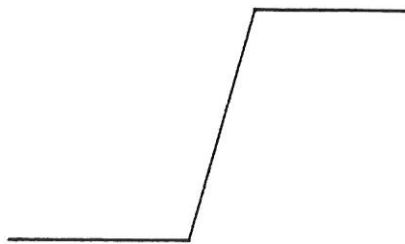


FIG. 3.1. Cross section of a step edge.

key concept in this paper. We will come back to this in the next section. First, we describe a simple heuristic method to create the edge classified image.

For each pixel (r, c) let $g_{\min}(r, c)$ and $g_{\max}(r, c)$ be the minimum and maximum graytone values in the set $\{P(x, y) | (x, y) \text{ is one of } (r, c)'s \text{ eight neighbors}\}$.

Next, calculate

$$\begin{aligned}\mu(r, c) &= (g_{\max}(r, c) + g_{\min}(r, c))/2, \\ \Delta(r, c) &= (g_{\max}(r, c) - g_{\min}(r, c))/2N,\end{aligned}$$

where N is a constant, to get different Δ values.

The C image is defined as

$$\begin{aligned}C(r, c) &= 1 && \text{if } P(r, c) \text{ is in } [g_{\min}(r, c), \mu(r, c) - \Delta(r, c)] \\ &&& \text{and } E(r, c) = 1, \\ &= 2 && \text{if } P(r, c) \text{ is in } [\mu(r, c) + \Delta(r, c), g_{\max}(r, c)] \\ &&& \text{and } E(r, c) = 1, \\ &= 0 && \text{otherwise.}\end{aligned}$$

If N is small and Δ is large, then fewer pixels will be classified as dark and bright edge pixels. Conversely, if N is large and Δ is small, then more pixels will be

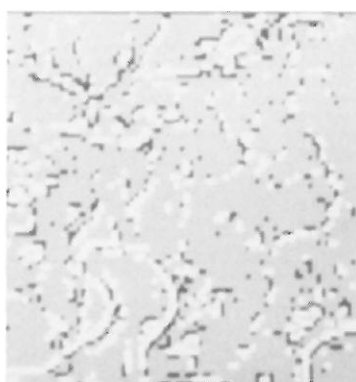
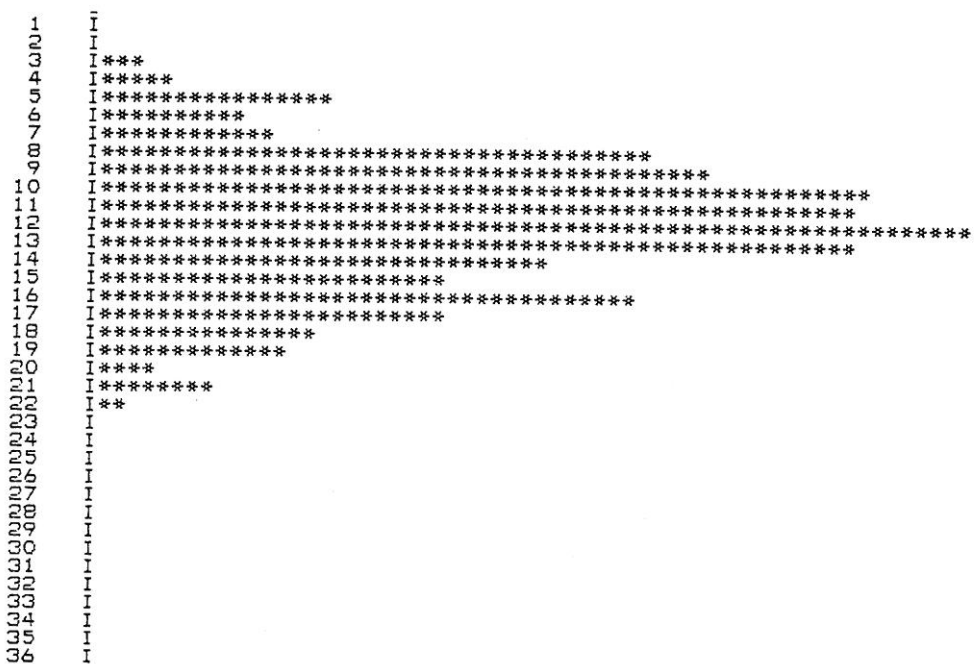
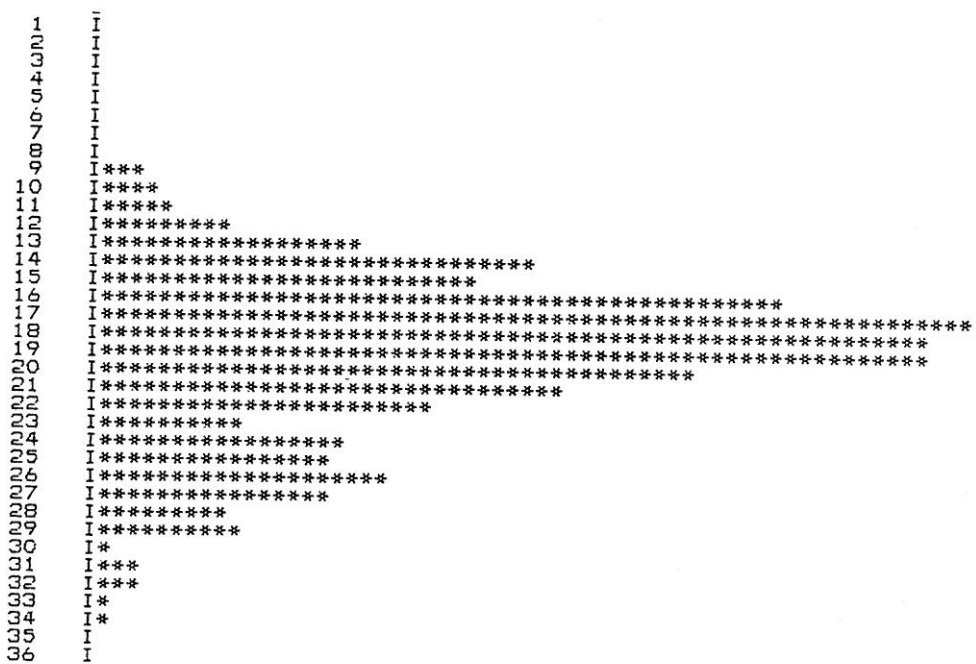


FIG. 3.2. Classified edge pixels of Fig. 2.3. Bright edge pixels are shown bright; dark edge pixels are shown dark.

FIG. 3.3a. Histogram H_d .FIG. 3.3b. Histogram H_b .

classified as dark and bright edge pixels. Thus we can get different C images by changing N . In most cases, N is set as 3. The classified edge image of the Landsat image is shown in Fig. 3.2, and the H_d , H_b histograms are shown in Fig. 3.3.

4. CRITERION FOR GOOD THRESHOLDS

The peak occurs at graytone 12 in H_d and occurs at graytone 17 in H_b for the Landsat image. Which one is a better threshold? Before looking at these two histograms in detail, let us study an ideal case as in Fig. 4.1, where region a is bright, region b is gray and region c is dark. Note that b is bright relative to c, but is dark relative to a. In terms of a classified edge image, b's edge pixels at the borders between b and c are bright edge pixels and b's edge pixels at the borders between a and b are dark edge pixels. Thus, in the graytone range of b's pixels, both the H_d and H_b histograms are expected to have significant population counts. Note also that c's edge pixels at the border between b and c are always classified as dark edge pixels, and that a's edge pixels at the border between a and b are always classified as bright edge pixels.

These observations correspond quite well to our definition of the P_k image in Section 1. The pixels with $P_k(r, c) = k$ will always be bright relative to the other pixels with $P_k \in [0, k - 1]$. The pixels with $P_k(r, c) = 0$ will always be dark relative to the pixels with $P_k \in [1, k]$. Also the pixels with $P_k(r, c) = i$, $i \in [1, k - 1]$ will be dark relative to pixels with $P_k \in [i + 1, k]$ and bright relative to pixels with $P_k \in [0, i - 1]$ at the same time.

Now we are ready to get some insight into H_d and H_b . Scan H_d and H_b from left to right. In the range $[1, 8]$, H_b has almost zero frequencies, but H_d does not. This means that if we threshold the image using $t \in [1, 9]$ to get dark regions, they are purely dark. Starting at graytone $g = 9$, the total population counts in the range $[1, g]$ are not zero in both H_d and H_b , which means that if we threshold the image using $t \in [10, 36]$, the dark regions we get are not so purely dark as if we use $t \in [1, 9]$. This suggests the definition of the probability of getting dark regions by

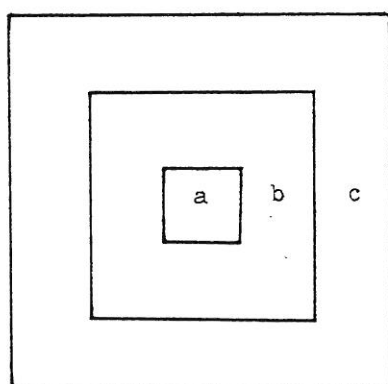


FIG. 4.1. An ideal image: region a is bright, region b is gray, and region c is dark.

FIG. 4.2a. Printout of $P_d(t)$: the probability of getting dark regions if thresholding at t .

A scatter plot showing the relationship between age (x-axis) and the number of children (y-axis). The x-axis ranges from 39 to 89, and the y-axis ranges from 1 to 36. The data points form a downward-sloping curve, indicating that as age increases, the number of children generally decreases.

Age	Number of Children
39	36
49	35
59	34
69	33
79	32
89	31

FIG. 4.2b. Printout of $P_b(t)$: the probability of getting bright regions if thresholding at t .

thresholding at t is

$$\begin{aligned}
 P_d(t) &= \frac{\text{Total population counts from } g_1 \text{ to } t \text{ for } H_d \text{ only}}{\text{Total population counts from } g_1 \text{ to } t \text{ for } H_d \text{ and } H_b} \times 100\% \\
 &= \frac{\sum_{i=g_1}^t H_d(i)}{\sum_{i=g_1}^t H_d(i) + \sum_{i=g_1}^t H_b(i)} \times 100\%
 \end{aligned}$$

Similarly, by scanning H_d and H_b from right to left, we can define the probability of

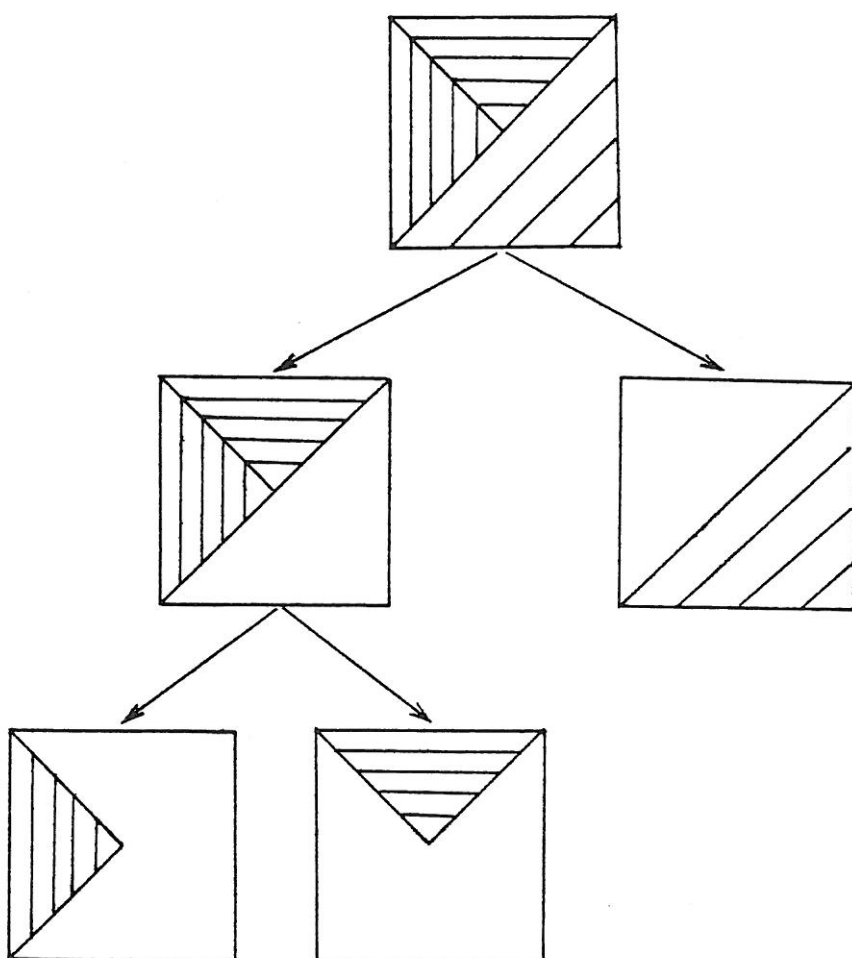
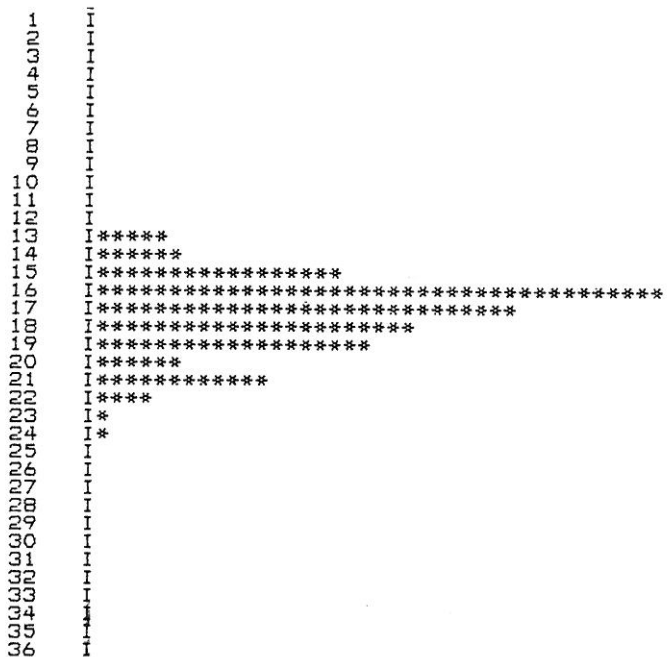
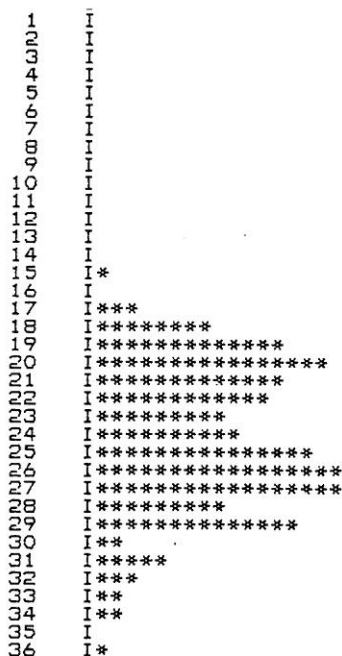
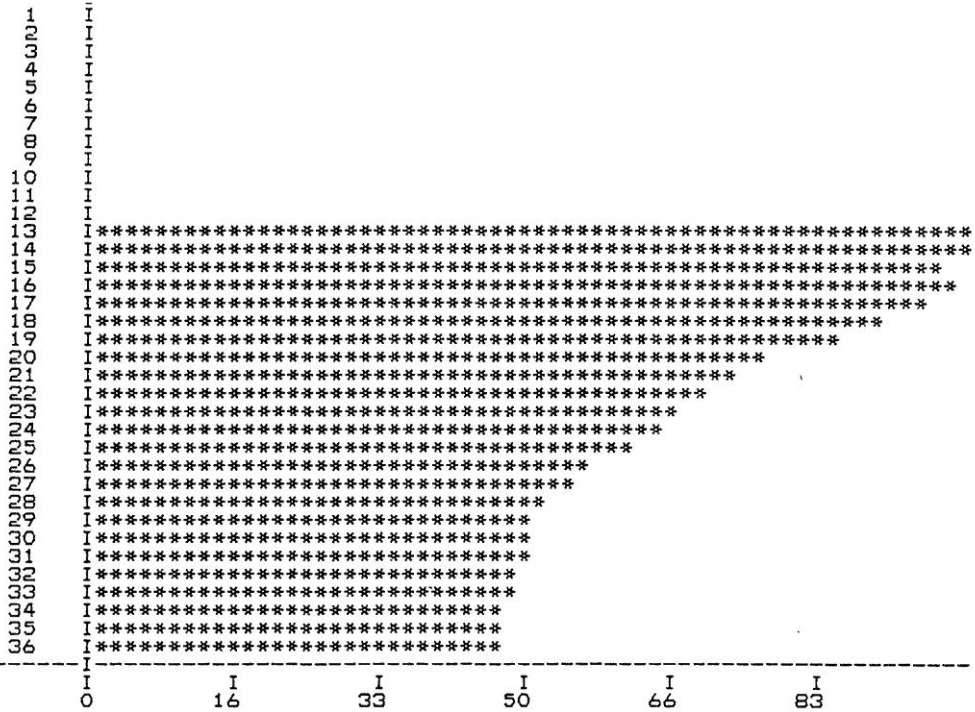
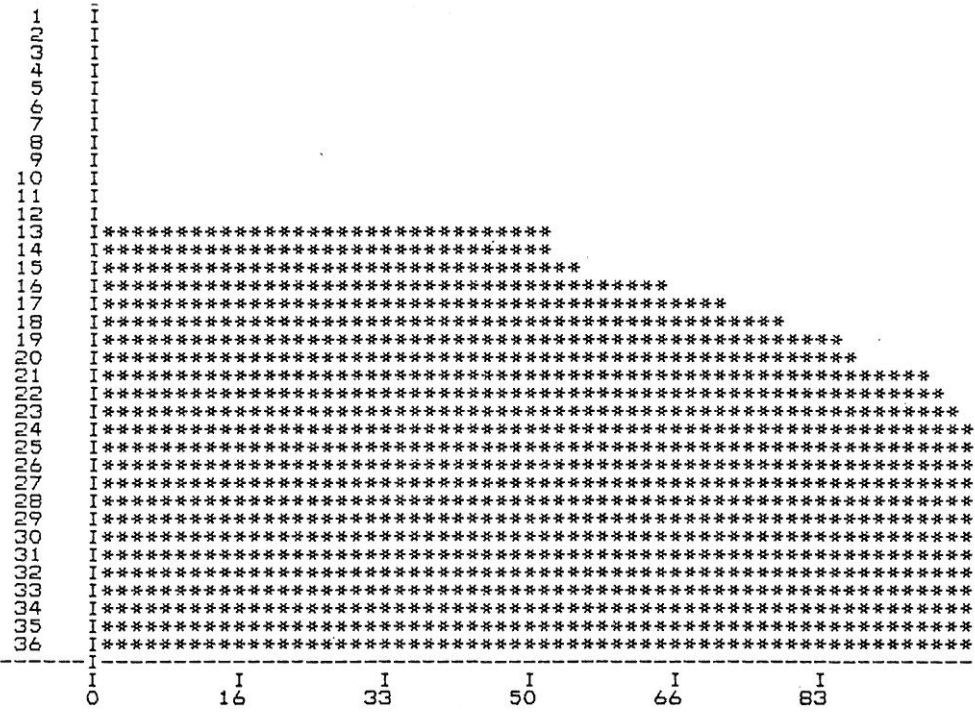


FIG. 5.1. An example of selecting two threshold values to separate three different regions.

FIG. 6.1a. H_d for graytone range [13, 36].FIG. 6.1b. H_b for graytone range [13, 36].

FIG. 6.1c. P_d for graytone range [13, 36].FIG. 6.1d. P_b for graytone range [13, 36].

```

1
2
3
4
5
6
7
8
9
10
11
12
13
14
15
16
17
18
19
20
21
22
23
24
25
26
27
28
29
30
31
32
33
34
35
36

```

FIG. 6.2a. H_d for graytone range [13, 25].

```

1
2
3
4
5
6
7
8
9
10
11
12
13
14
15
16
17
18
19
20
21
22
23
24
25
26
27
28
29
30
31
32
33
34
35
36

```

FIG. 6.2b. H_b for graytone range [13, 25].

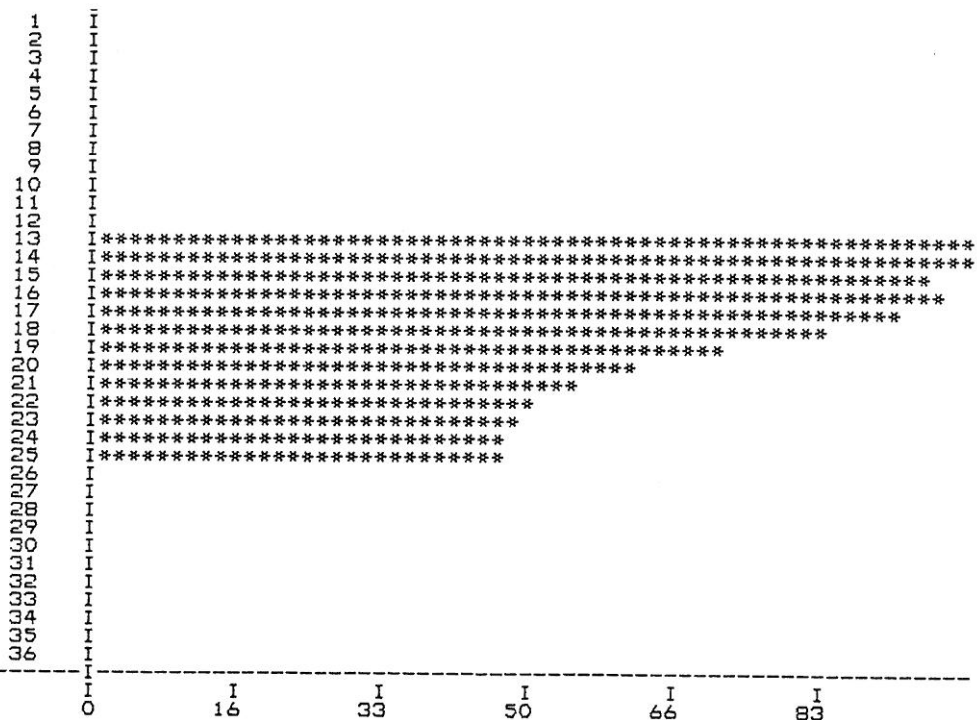
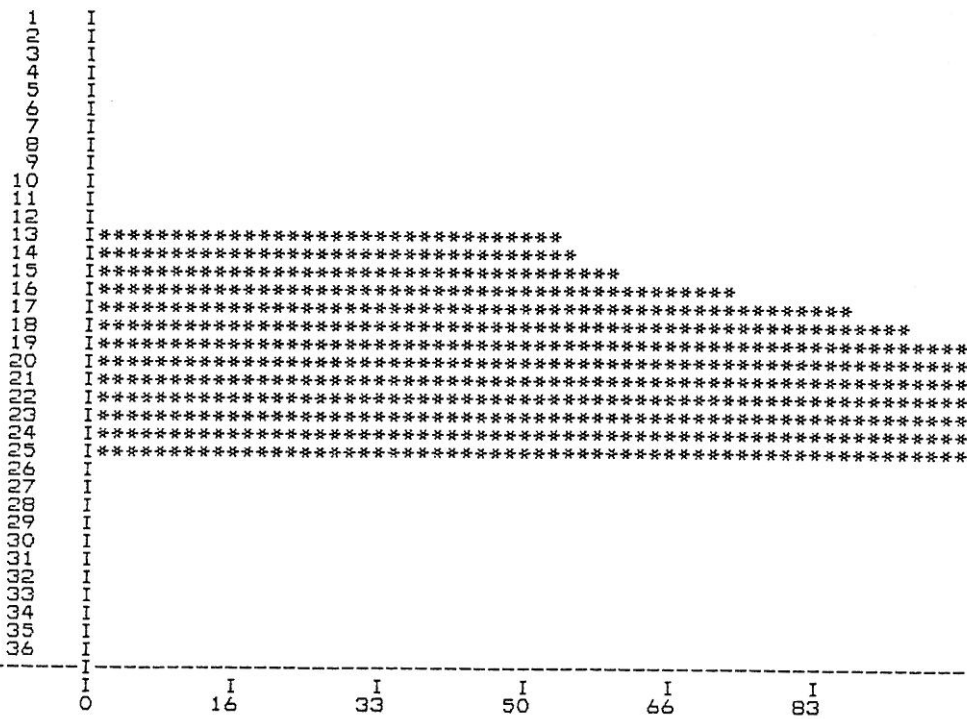
FIG. 6.2c. P_d for graytone range [13, 25].FIG. 6.2d. P_b for graytone range [13, 25].



FIG. 6.3. Sliced binary image for graytone range [1, 12].

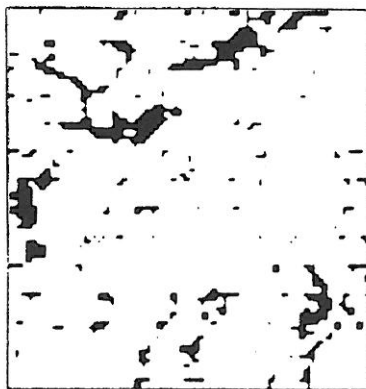


FIG. 6.4. Sliced binary image for graytone range [20, 36].

getting bright regions by thresholding at t as

$$P_b(t) = \frac{\sum_{i=t}^{g_2} H_b(i)}{\sum_{i=t}^{g_2} H_d(i) + \sum_{i=t}^{g_2} H_b(i)}.$$

Figure 4.2 shows the printout of P_d and P_b with respect to graytone values for the Landsat image. Because $P_d(12)$ is higher than $P_b(17)$, 12 is selected as the threshold value. In general, the rule is

Rule. If the peak of H_d occurs at g_d and the peak of H_b occurs at g_b , and $P_d(g_d) \geq P_b(g_b)$, then g_d is selected as the threshold. Conversely, if $P_d(g_d) < P_b(g_b)$, g_b is selected as the threshold.

5. RECURSIVE MULTITHRESHOLD SELECTION

Using the threshold value selected by the rule in the last section, we can get one image of bright regions and another image of dark regions. Repeating the steps for

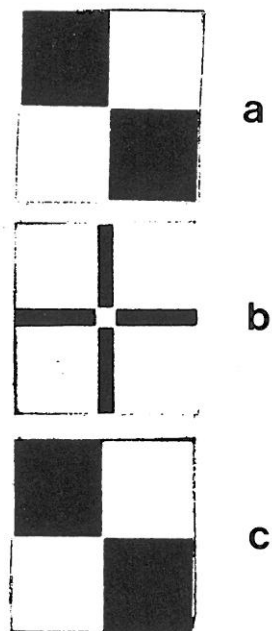


FIG. 6.5. (a) Perfect checkerboard for graytone range [10,15]. (b) Edge image. (c) Sliced binary image for graytone range [10,10].

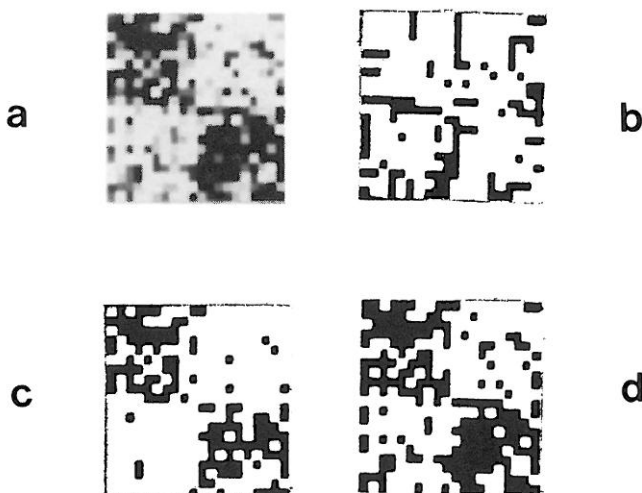


FIG. 6.6. (a) Noisy checkerboard for graytone range [10,15]. (b) Edge image. (c) Sliced binary image for graytone range [10,10]. (d) Sliced binary image for graytone range [10,12].

these two new images, we can get other images of even brighter or darker regions. This is exactly the same idea Ohlander [8] used in his recursive segmentation method. A similar method was devised by Milgram and Kahl [9] who used the concept of convergent evidence to accept or reject object regions in recursive region extraction. Milgram and Herman [10] discuss convergent evidence from clustering thinned edge points in a 2-D histogram using gray level value and edge value as axes. An example of the recursive thresholding method is shown in Figure 5.1.

In the implementation, we do not need to actually create the new images during the selection of thresholds. Instead, we can keep on reducing the graytone range $[g_1, g_2]$ as the thresholding removes either the most bright or the most dark regions. Thus, the algorithm is

```

Initially,  $g_1 \leftarrow$  actual minimum graytone in image  $P$ ,  

         $g_2 \leftarrow$  actual maximum graytone in image  $P$ ,  

         $j \leftarrow 0$ .  

Repeat  

begin:  $j \leftarrow j + 1$   

    Create  $H_d$ ,  $H_b$   

    If the total population counts in either  $H_d$  or  $H_b$  are not  

    significant, stop.  

    Use the rule in Section 4 to select  

    threshold  $t(j)$  in  $[g_1, g_2]$ .  

    If  $t(j) = g_d$  then  $g_1 \leftarrow g_d + 1$   

    If  $t(j) = g_b$  then  $g_2 \leftarrow g_b - 1$   

end.

```

6. EXPERIMENTAL RESULTS

Let us continue with the Landsat image example. After $g_d = 12$ is selected as the first threshold, the graytone range is reduced to $[13, 36]$. The printouts of H_d , H_b , P_d , P_b for this range are shown in Fig. 6.1. $g_b = 26$ is selected as the next threshold, and the graytone range is reduced to $[13, 25]$. The printouts of H_d , H_b , P_d , P_b for this new range are shown in Fig. 6.2. $g_b = 20$ is selected as the next threshold, and the graytone range is reduced to $[13, 19]$. Since the total population counts for H_d and H_b are not significant, the algorithm stops.

Instead of showing the $(k + 1)$ -valued image P_k , we show the binary sliced image for each graytone range, i.e., for a graytone range $[g_x, g_y]$, sliced image S : $Z_r \times Z_c \rightarrow \{0, 1\}$ is defined as

$$\begin{aligned} S(r, c) &= 1 && \text{if } g_x \leq P(r, c) \leq g_y \\ &= 0 && \text{otherwise.} \end{aligned}$$

The sliced image for $[1, 12]$ is shown in Fig. 6.3, and the sliced image for $[20, 36]$ is shown in Fig. 6.4. The regions in Fig. 6.3 represent shadows, and the regions in Fig. 6.4 represent vegetated area. The explanations are given in Wang *et al.* [11]. Because the sliced image for $[26, 36]$ is just a subset of Fig. 6.4, we do not show it.

Experiments were done for a variety of other images such as a checkerboard, a noisy checkerboard, a chair, and a house. The original images, edge images, and sliced images are shown in Figs. 6.5 to 6.8.

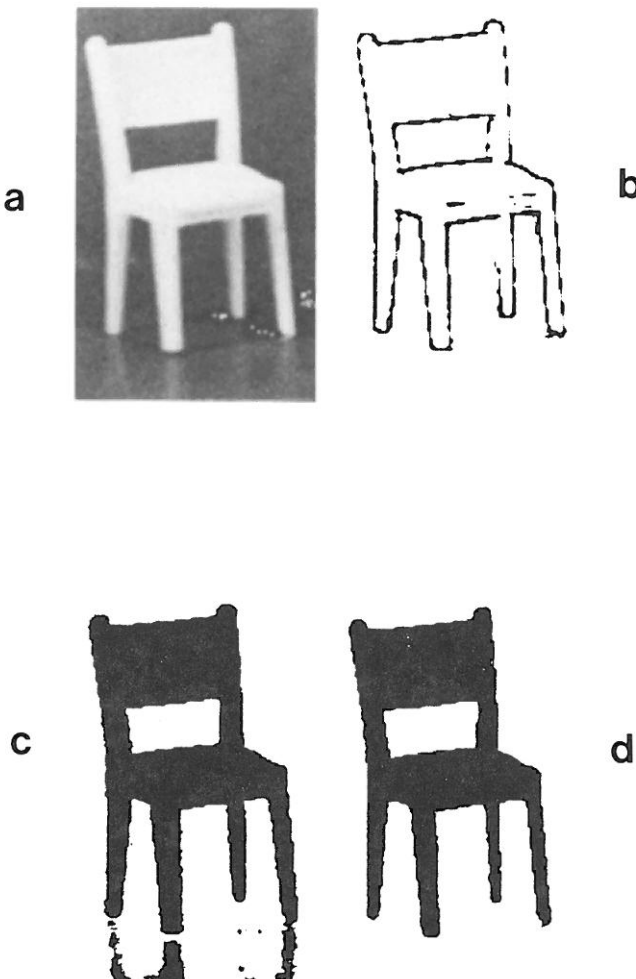


FIG. 6.7. (a) Chair image. (b) Edge image. (c) Sliced binary image for graytone range [124, 255]. (d) Sliced binary image for graytone range [140, 255].

7. DISCUSSION

For the Landsat image, the peak of H_1 occurs at the graytone 16. By Watanabe's method, this would be selected as threshold. However, in our method, 12, 20, and 26 are selected as thresholds, and 16 is never selected because it is not compatible with the others in getting pure bright or dark regions.

Reasonable results are obtained in the last section for several quite different images, which indicates that the approach is quite general.

REFERENCES

1. J. S. Weszka, A survey of threshold selection techniques, *Computer Graphics Image Processing* 7, 1978, 259–265.
2. S. Watanabe et al., An automated apparatus for cancer prescreening: CYBEST, *Computer Graphics Image Processing* 3, 1974, 350–358.

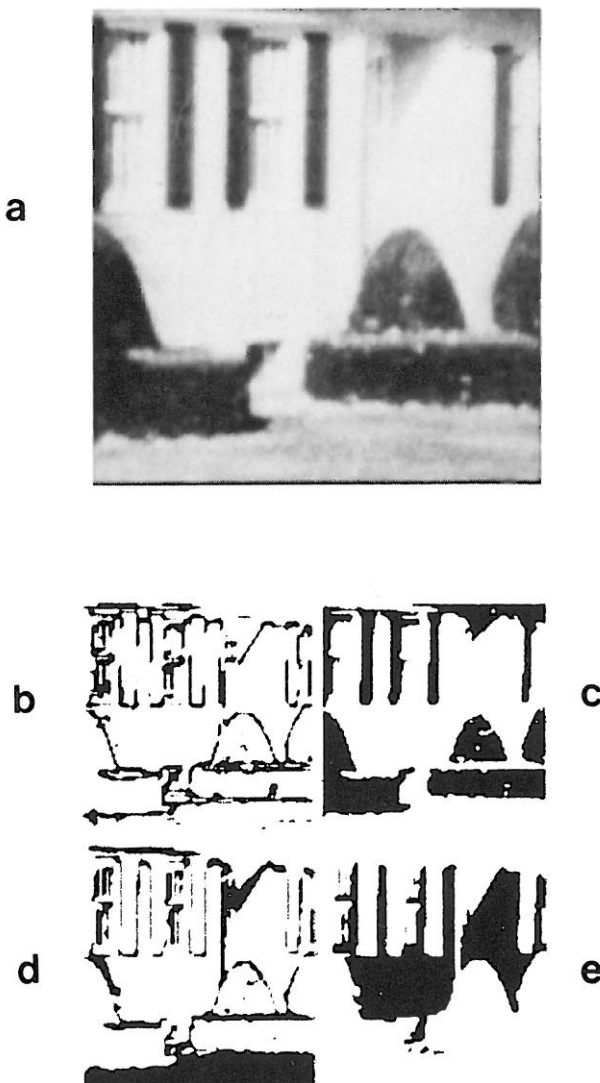


FIG. 6.8. (a) House image. (b) Edge image. (c) Sliced binary image for graytone range [1, 116]. (d) Sliced binary image for graytone range [117, 191]. (e) Sliced binary image for graytone range [192, 255].

3. C. K. Chow and T. Kaneko, Boundary Detection of Radiographic Images by a Threshold Method, Proceedings, IFIP Congress 71, Booklet TA-7, pp. 130-134, 1972.
4. J. S. Weszka, J. A. Verson, and A. Rosenfeld, Threshold Selection Techniques-2, TR-260, Computer Science Center, University of Maryland, 1973.
5. J. S. Weszka and A. Rosenfeld, Histogram modification for threshold selection, *IEEE Trans. Syst. Man Cybern. SMC-9*, 1979.
6. Y. H. Katz, Pattern Recognition of Meteorological Satellite Cloud Photography, Proceedings, 3rd Symposium on Remote Sensing of Environment, pp. 173-214, University of Michigan, 1965.
7. R. M. Haralick, Zero-Crossing of Second Directional Derivative Edge Operator, Proceedings of the Society of Photo-Optical Instrumentation Engineers Technical Symposium, Vol. 336-23, East Arlington Va., May 1982.

8. R. B. Ohlander, *Analysis of Natural Scenes*, Ph.D. dissertation, Dept. of Computer Science, Carnegie-Mellon University, 1975.
9. D. L. Milgram and D. J. Kahl, Recursive region extraction. *Computer Graphics Image Processing* **9**, 1979, 82-88.
10. D. L. Milgram and M. Herman, Clustering edge values for threshold selection, *Computer Graphics Image Processing* **10**, 1979, 272-280.
11. S. Wang, D. B. Elliott, J. Campbell, R. W. Ehrich, and R. M. Haralick, Spatial Reasoning in Remotely Sensed Data, Technical Report, Dept. of Computer Science, Virginia Polytechnic Institute, 1981.